Supporting information for:

Enhanced CO2 Sorption Properties in a Polarizable [WO2F4]2-- Pillared Physisorbent under Direct Air Capture Conditions

Daniel O'Nolan, Lindsey Chatterton, Timothy Bellamy, J. Todd Ennis, Mustapha Soukri*

RTI International, Research Triangle Park, NC 27709-2194, USA

*Corresponding author: msoukri@rti.org

Materials and Procedures

All reagents were purchased from commercial and used as received without further purification. All gases used throughout this work were of ultrahigh purity grade.

Powder X-ray Diffraction

X-ray diffraction data suitable for structure solution was collected on a Bruker D8 Advance diffractometer in Bragg-Brentano geometry with a Cu kα source (1.54051 Å, 40 kV, 40 mA) and Lynxeye XE-T detector. A continuous-scan collection strategy was used in the range 5° < 2θ < 120° with a step size of 0.01° and rate of 0.1 °/min. Data was fitted, solved *via* charge-flipping, and refined using the Rietveld method as implemented in GSAS-II (v5002).

In situ X-ray diffraction analysis was carried out on a PANalytical XPert Pro mounted with an Anton Paar XRK-900 reaction chamber. Data was collected in Bragg-Brentano geometry with a Cu kα source (1.54251 Å, 45 kV, 40 mA) and PIXcel 1D detector. A 6 min continuous-scan collection strategy was used in the range 5.01° < 2θ < 60° with a step size of 0.01°. Temperature was ramped to 393 K at 10 K min-1 and held at that temperature for 1 hour, before being cooled back to room temperature. Diffraction scans were repeatedly collected throughout the experiment.

Miller indices associated with the organic axes (h00 / hk0 / hkl) were observed to expand upon heating and then contract to their initial position upon cooling (**Figure S1**). Indices associated with the inorganic axis (00l / hhl) were observe to contract upon heating and remain in that position upon cooling. In contrast, the h0l indices were found to exhibit either phenomenon depending on the magnitude of h and l (h > l: expands upon heating, contracts upon cooling; l > h: contacts upon heating and remains in new position upon cooling). This is a result of the organic/inorganic axis' influence on those planes (**Figure S2**).

Fourier Transform Infrared Spectroscopy (FT-IR)

FT-IR data was collected on a Perkin Elmer Spectrum 100 with a universal Attenuated Total Reflectance (UATR) sample mount. Data was collected on pristine microcrystalline samples in the range 4000 – 400 cm^{-1} with a step size of 4 cm^{-1} with a total of 4 scans each (**Figure S3**).

Gas Sorption Analysis

Volumetric gas sorption data was collected on a Micromeritics ASAP 2020 (v4.03) using *ca.* 0.134 g of material. Samples were evacuated overnight under dynamic vacuum at 120 ℃. N_2

(77 K) and CO_2 (273 K, 283 K, 298 K) adsorption data was collected in the low-pressure region (up to 1 bar).

Gravimetric gas sorption data was carried out on a Hiden Isochema Intelligent Gas Analyzer (IGA) connected to a Hiden Analytical DSMS mass spectrometer. Gases were dried *via* molecular sieve (5A) moisture traps and controlled using mass flow controllers.

Samples were activated *via* heating to 80 ℃ for 1.5 hours (including ramp) under N_2 flow. For experiments carried out in the presence of water vapor, relative humidity was controlled by saturating a flow of house N_2 gas (from cryogenic boil-off). This humid line was then blended with a dry N_2 line and a 1% CO_2/99% Air line to afford the desired humidity. The flow of the 1% CO_2 line was further controlled to afford 400 ppm CO_2 concentration at the outlet (**Figure S4**). The vapor generator and extending lines were temperature kept isothermal, as was the sample reactor, using recirculating water. The temperature of both the vapor generator and sample reactor were set to the same temperature to ensure the correct vapor pressure of water.

After activation, the sample was exposed to the gas mixture and the change in sample mass was recorded over time. The CO_2 capacity was evaluated using the combined gravimetric and dynamic sample mass spectrometry as described by Fletcher *et al.* (*J. Phys. Chem. B*, **2002**, 106, 30, 7474-7482). The sample was regenerated at 80 ℃ for 1.5 hours (including ramp) and the temperature programmed desorption of CO_2 and H_2O was recorded using mass spectrometry. N_2 is treated as a non-adsorbing gas given the negligible uptake at 77 K. The concentration of the two gases were converted to mass and their ratio was compared with that of the total adsorbed mass to determine the total CO_2 capacity of the sample.

Isosteric enthalpies of adsorption were estimated using the Clausius-Clapeyron equation as implemented in PyGAPs (Iacomi, P. and Llewellyn, P. L. *Adsorption*, **2019**, 25, 1533-1542). Volumetric isothermal adsorption data ($1x10^{-4}$ bar – 1 bar, 273K, 283 K, and 298K) was fitted with a Dual-Site Langmuir Isotherm. Gravimetric isothermal adsorption data was collected in the range $0.007 < p/p0 < 0.043$ (293 K, 298 K, 303 K). These linear adsorption profiles were fitted with Henry's equation. Ideal Adsorbed Solution Theory calculations were calculated using the same isotherms and fittings. Selectivities were calculated for DAC (CO_2 p/p_0 = 0.04%), ambient room concentrations (ca. 1% CO_2), natural gas combined cycle concentrations (ca. 4% CO_2) and flue gas concentrations (ca. 15% CO_2). Additionally, CO_2/CH_4 selectivity calculations were determined for different natural gas processes (1%, 5%, and 50% CO_2). These results are shown in **Figures S6-S19** and **Table 2**. The Jupyter notebooks are attached as a .pdf.

Table S1. Crystallographic Information for WO_2F_4-1-Ni

Formula	$\{[(WO_2F_4)Ni(C_4H_4N_2)_2]\cdot 2H_2O\}_n$
Crystal Density / g cm^{-3}	2.4783
a = b / Å	9.91785(6)
C /Å	15.71517(9)
α = β = γ / °	90.0
Volume / $Å^3$	1545.80(2)
Space Group	*I4* / *mcm*
Observations (Reflections)	11187 (331)
wR	0.1062
R	0.0718
Rbackground	0.0980
wRmin	0.0066
RF	0.0671
RF^2	0.1266
GoF	16.03
Geometry	Bragg-Brentano
Scanning Range	$5.01 \leq 2\theta \leq 120.00$

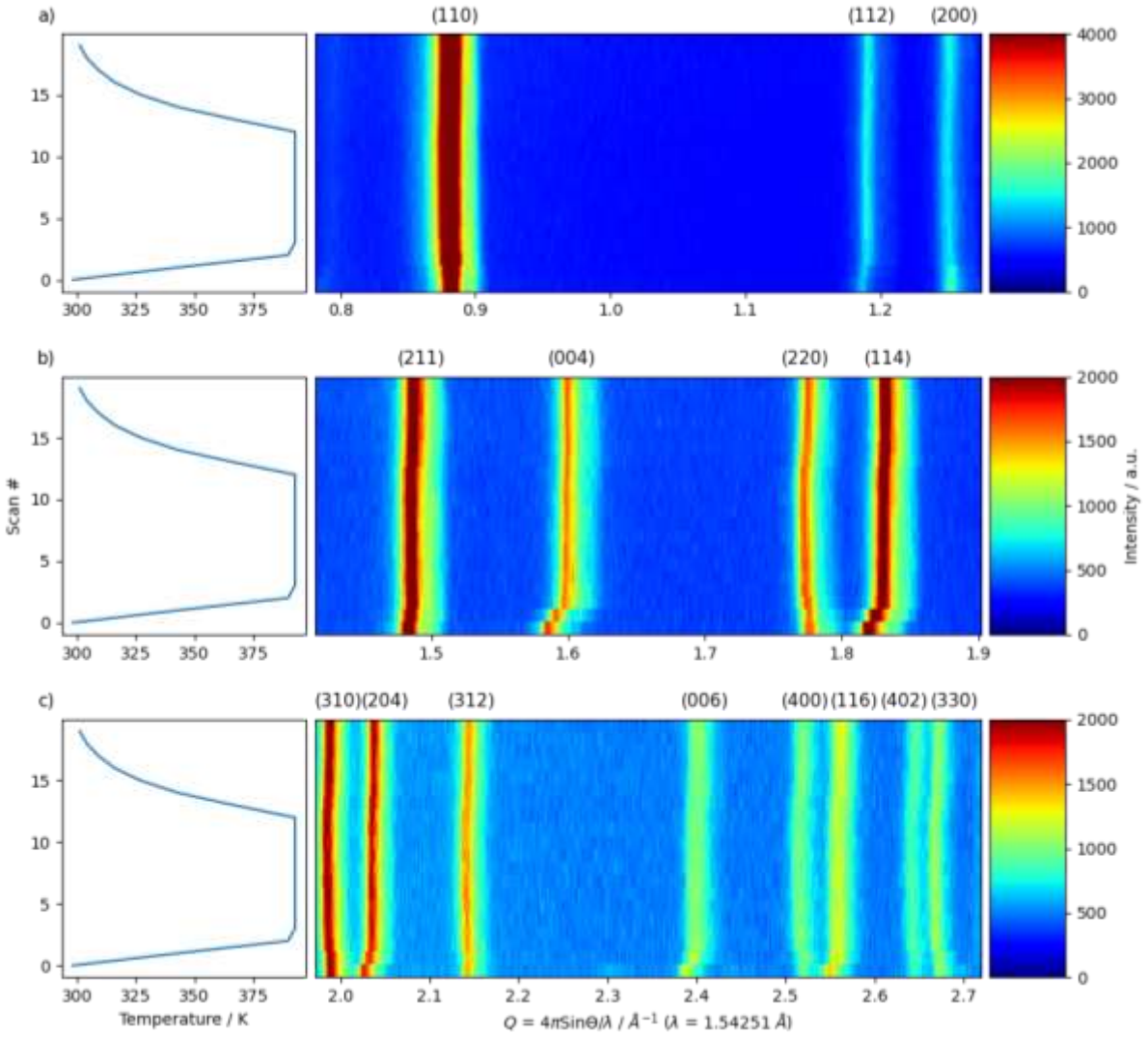

Figure S1. *In situ* powder X-ray diffraction data demonstrating the expansion/contraction of peaks upon activation of WO_2F_4-1-Ni.

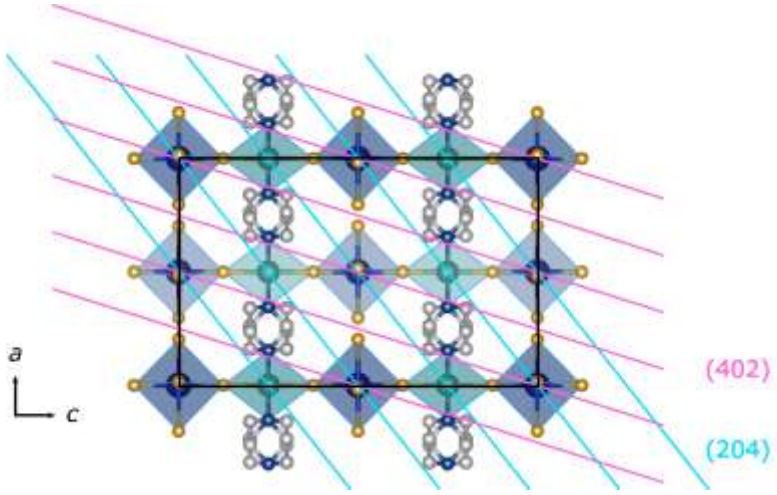

Figure S2. Representation of expanding and contracting planes (*h0l*) in WO_2F_4-1-Ni.

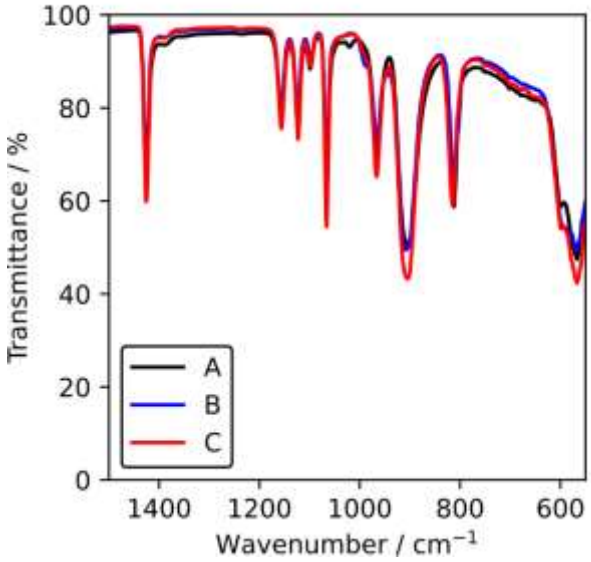

Figure S3. FT-IR spectra of different WO_2F_4-1-Ni batches.

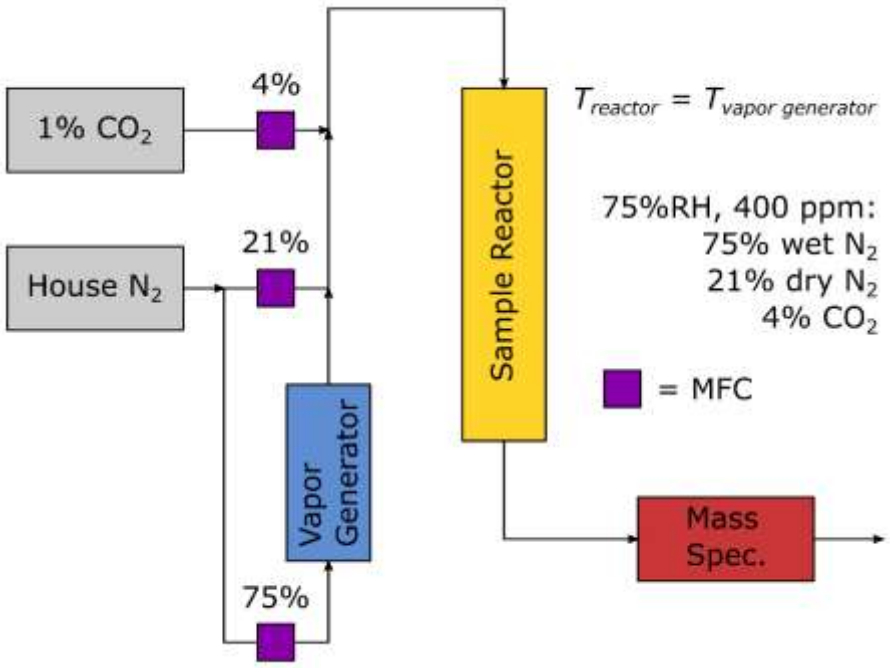

Figure S4. Layout of gas flow during a dynamic gravimetric adsorption experiment. Vapor generator is isothermal with reactor.

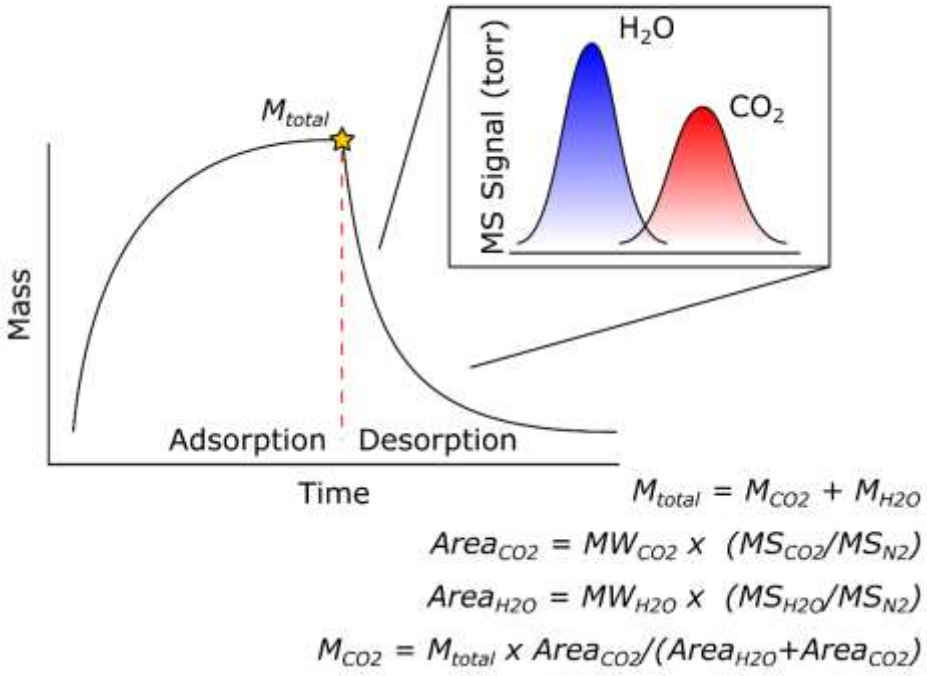

Figure S5. Description of the combined gravimetry and dynamic sampling mass spectrometry approach to evaluate the CO_2 capacity of materials under multicomponent adsorption experiments.

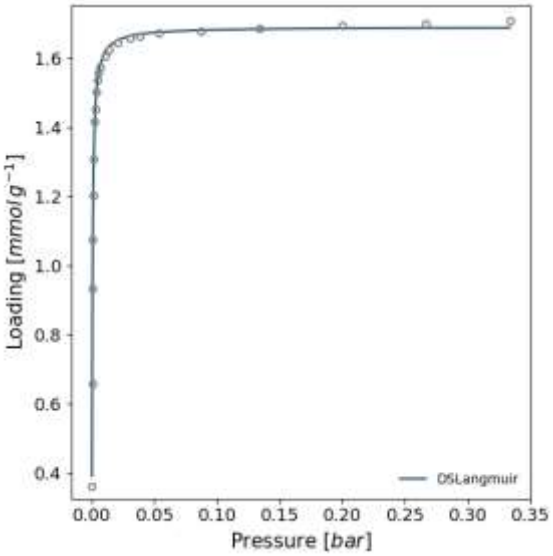

Figure S6. Dual-Site Langmuir fitting (RMSE = 0.0126, m1 = 0.7787, m2 = 0.9119, K1 = 1276, K2 = 5278) to 298 K CO_2 adsorption isotherm on WO2F4-1-Ni.

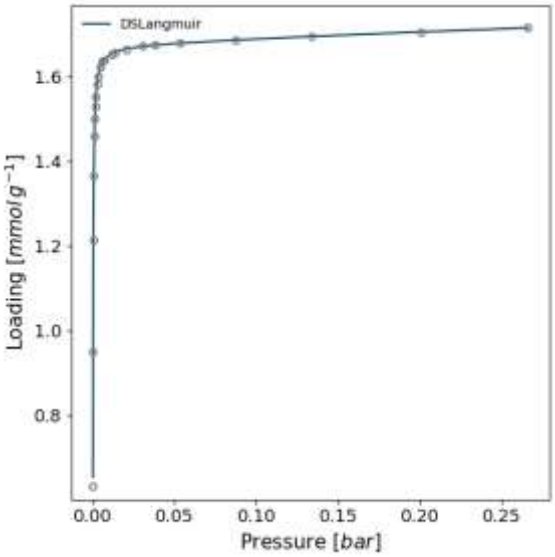

Figure S7. Dual-Site Langmuir fitting (RMSE = 0.00571, m1 = 0.3129, m2 = 1.673, K1 = 0.5801, K2 = 6718) to 283 K CO_2 adsorption isotherm on WO2F4-1-Ni.

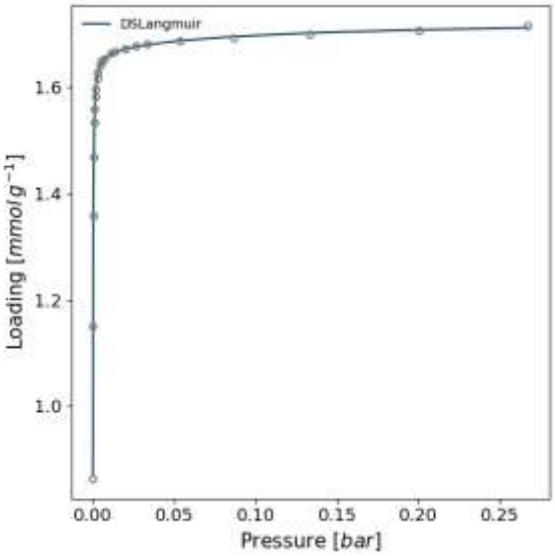

Figure S8. Dual-Site Langmuir fitting (RMSE = 0.0039, m1 = 0.5856, m2 = 1.669, K1 = 10.6, K2 = 1.14E+04) to 273 K CO_2 adsorption isotherm on WO2F4-1-Ni.

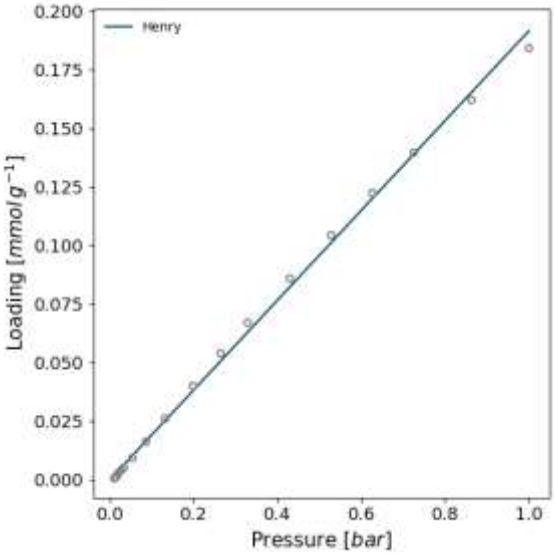

Figure S9. Henry fitting (RMSE = 0.00192, K = 0.1288) to 298 K N2 adsorption isotherm on WO2F4-1-Ni.

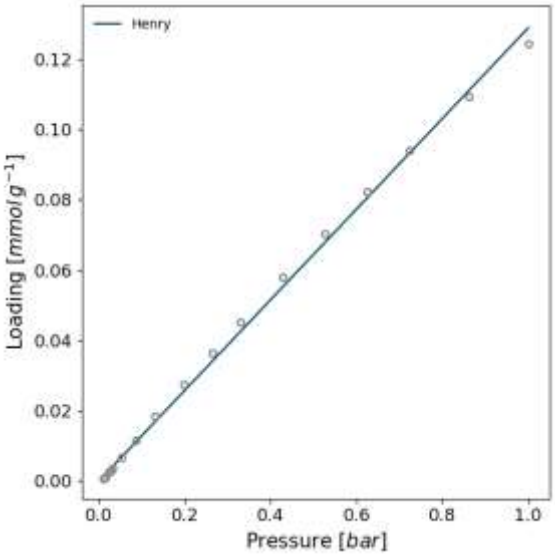

Figure S10. Henry fitting (RMSE = 0.00291, K = 0.1917) to 298 K CH_4 adsorption isotherm on WO2F4-1-Ni.

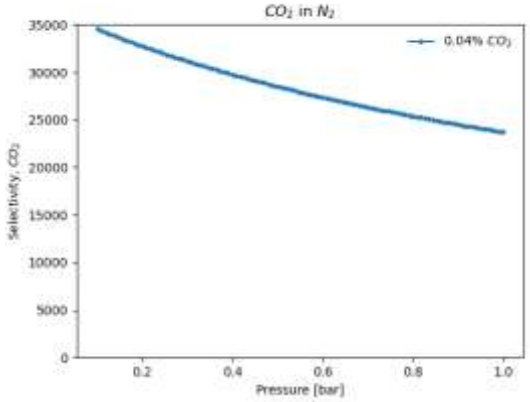

Figure S11. CO_2/N_2 selectivity as a function of pressure on WO2F4-1-Ni at 298 K. The concentration of CO_2 is 0.04%, or 400 ppm, with N_2 as balance. Selectivity at 1 bar pressure is relevant to ambient direct air capture (DAC) conditions.

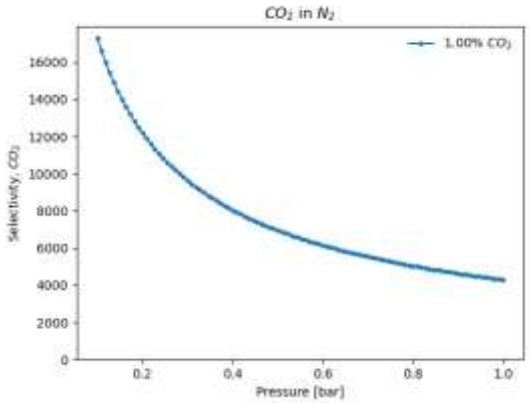

Figure S12. CO_2/N_2 selectivity as a function of pressure on WO2F4-1-Ni at 298 K. The concentration of CO_2 is 1% with N_2 as balance. The gas composition represented here is relevant to ambient room conditions.

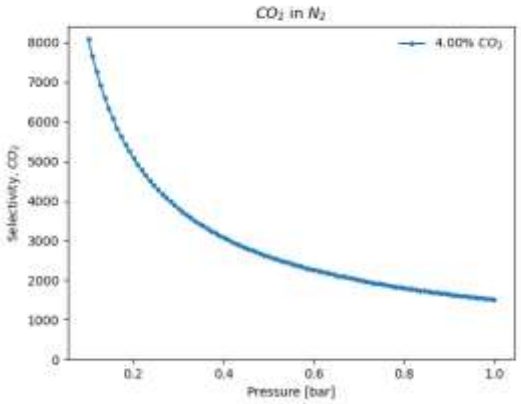

Figure S13. CO_2/N_2 selectivity as a function of pressure on WO2F4-1-Ni at 298 K. The concentration of CO_2 is 4% with N_2 as balance. The gas composition represented here is relevant to natural gas combined cycle (NGCC) conditions.

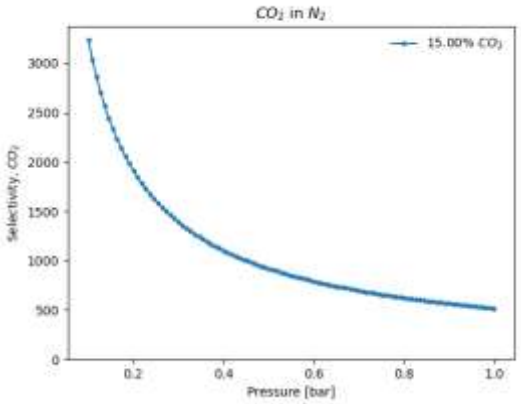

Figure S14. CO_2/N_2 selectivity as a function of pressure on WO2F4-1-Ni at 298 K. The concentration of CO_2 is 15% with N_2 as balance. The gas composition represented here is relevant to typical flue gas conditions.

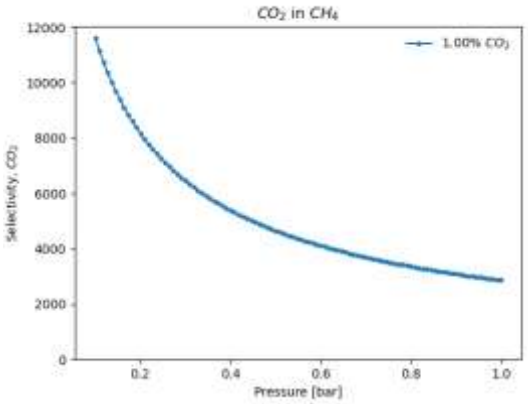

Figure S15. CO_2/CH_4 selectivity as a function of pressure on WO2F4-1-Ni at 298 K. The concentration of CO_2 is 1%, or 400 ppm, with N_2 as balance.

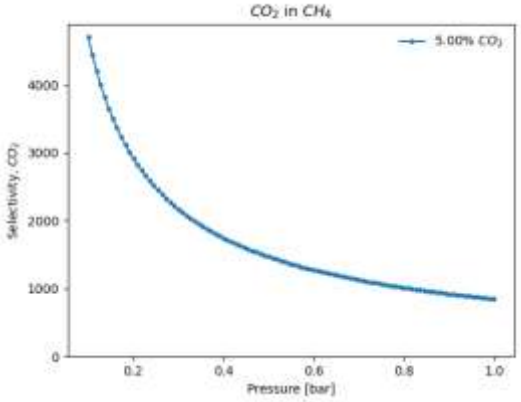

Figure S16. CO_2/CH_4 selectivity as a function of pressure on WO2F4-1-Ni at 298 K. The concentration of CO_2 is 5% with N_2 as balance.

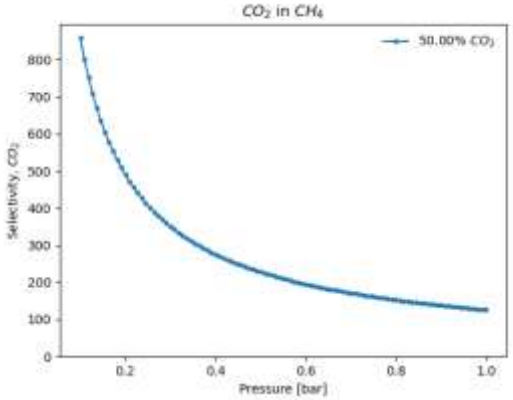

Figure S17. CO_2/CH_4 selectivity as a function of pressure on WO2F4-1-Ni at 298 K. The concentration of CO_2 is 50% with N_2 as balance.

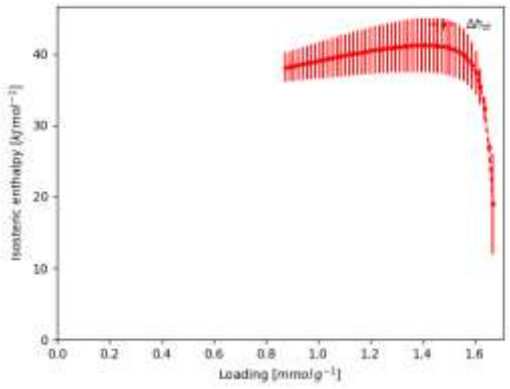

Figure S18. CO_2 Isosteric enthalpy of adsorption as a function of loading in WO_2F_4-1-Ni.

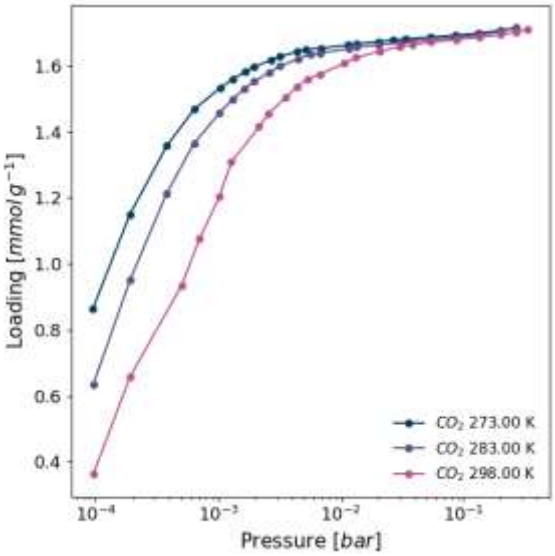

Figure S19. Log plot comparison of CO_2 adsorption isotherms for WO_2F_4-1-Ni at different temperatures.

Table S2. IAST selectivity $S_{a/b}$ for a = CO_2

Process	*b*	CO_2 conc.	$S_{a/b}$ (1 bar, 298K)
DAC	N_2	0.04%	23711.40
Room	N_2	1%	4288.31
NGCC	N_2	4%	1510.47
Flue	N_2	15%	517.39
NG Process	CH_4	1%	2858.93
	CH_4	5%	845.72
	CH_4	50%	125.85

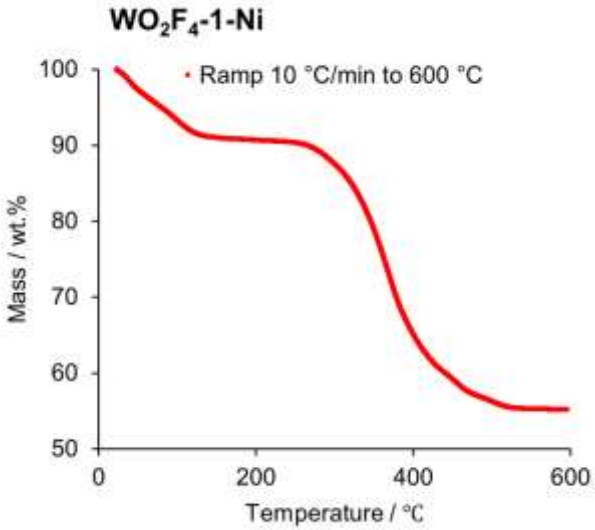

Figure S20. TGA thermogram of WO_2F_4-1-Ni.

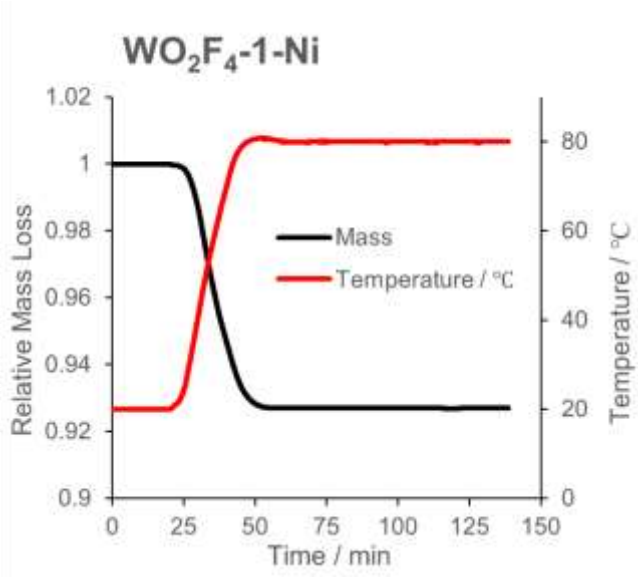

Figure S21. CO_2/H_2O temperature programmed desorption profile from WO_2F_4-1-Ni.

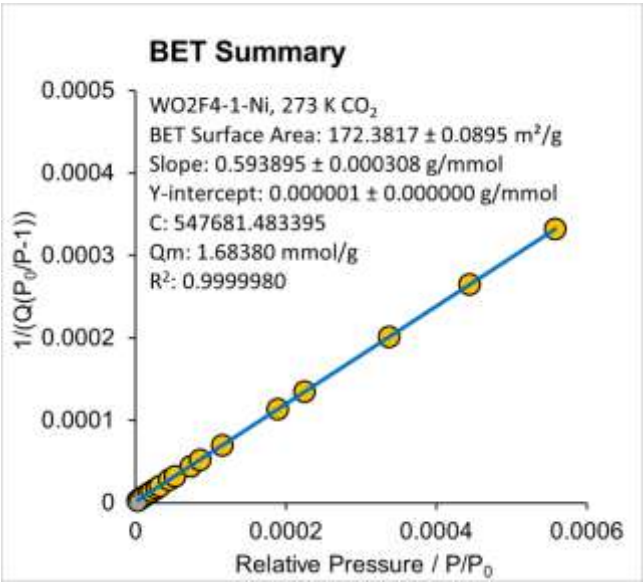

Figure S22. BET Summary for WO_2F_4-1-Ni, using 273 K CO_2 sorption data.

Table S3. Raw Material Cost Evaluation for metals used as anionic pillars.

Metal	Source	Metal Mass Conc.	Cost	Ref.
Tungsten (W)	WO_3	79 %	$28 / Kg	https://www.metal.com/Tungsten/202209270001 (Accessed: Aug 8, 2023)
Niobium (Nb)	Nb_2O_5	69.9 %	$53 / Kg	https://www.metal.com/Niobium-Tantalum/202211090009 (Accessed: Aug 8, 2023)